



# Evaluation of the Physicochemical and Thermal Properties of Chromium Trioxide ( $\text{CrO}_3$ ): Impact of Consciousness Energy Healing Treatment



Gopal Nayak<sup>1</sup>, Mahendra Kumar Trivedi<sup>1</sup>, Alice Branton<sup>1</sup>, Dahryn Trivedi<sup>1</sup> and Snehasis Jana<sup>2,\*</sup>

<sup>1</sup>Trivedi Global, Inc, Henderson, USA

<sup>2</sup>Trivedi Science Research Laboratory Pvt, India

\*Corresponding author: Snehasis Jana, Bhopal, India

Submission:  September 24, 2018; Published:  October 29, 2018

## Abstract

Chromium trioxide ( $\text{CrO}_3$ ) has many industrial applications for the manufacturing of aerospace parts, synthetic rubies, stripping agent, etc. but it is very hygroscopic, toxic and powerful oxidizing material. The objective of this study was to evaluate the influence of the Trivedi Effect®-Consciousness Energy Healing Treatment on the physicochemical and thermal properties of  $\text{CrO}_3$  using modern analytical techniques. The sample was divided into two parts, one part of the test sample was considered as the control sample (no Biofield Treatment was provided), while another portion received the Biofield Treatment remotely by a renowned Biofield Energy Healer, Gopal Nayak and termed as the treated sample. The particle size values of the treated  $\text{CrO}_3$  were increased by 2.39%, 4.52%, 4.42%, and 4.15% at  $d_{10}$ ,  $d_{50}$ ,  $d_{90}$ , and  $D(4,3)$ , respectively compared to the control sample. Thus, the specific surface area of the treated  $\text{CrO}_3$  was decreased by 4.27% compared with the control sample. The PXRD peak intensities of the treated  $\text{CrO}_3$  were significantly altered ranging from -73.48% to 212.5% compared with the control sample. Similarly, the crystallite sizes of the treated sample were significantly altered ranging from -38.7% to 167.39% compared to the control sample. However, the average crystallite size of the treated sample was increased by 4.25% compared with the control sample. The latent heat of fusion of the treated sample was significantly increased by 556.45% compared with the control sample. The Trivedi Effect®-Consciousness Energy Healing Treatment might produce a new polymorphic form of  $\text{CrO}_3$  which would be better powder flowability and lower solubility; hence it will show the lower absorption and toxicity on inhalation, ingestion, contact to skin and eye, chronic exposure, and aggravation of pre-existing conditions. The Biofield Energy Treated  $\text{CrO}_3$  sample would be very useful for the ceramic industry manufacturing the synthetic rubies, stripping agent of anodic coatings, aerospace parts, etc.

**Keywords:** Chromium trioxide; Trivedi effect®; Consciousness energy healing treatment; Complementary and alternative medicine; Particle size; Surface area; Crystallite size; DSC

## Introduction

Chromium (VI) oxide (chromium trioxide;  $\text{CrO}_3$ ) is an acidic anhydride of chromic acid [1]. Chromium oxide is highly hygroscopic and a powerful oxidizer. Being a powerful oxidizer, it will ignite the organic materials on contact (i.e., alcohol) [2]. It is typically applied for the chrome plating and it generates passivating chromate films by reacting with cadmium, zinc, and other metals to protect from the process of corrosion [3]. Aerospace parts, synthetic rubies, and stripping agent of anodic coatings also manufactured from chromium oxide [2,4]. Chromium oxide is highly corrosive, toxic, and carcinogenic. It causes potential damage to the health through inhalation, ingestion, contact with the eye and skin, chronic exposure, and aggravation of pre-existing conditions [5].

Characterization of the physicochemical properties is attained a strong interest in the different field of the scientific research area and is now a standard method, which is one of the key challenges developing an object with the appropriate physicochemical profile. The Trivedi Effect®-Biofield Energy Healing Treatment is an

economically viable approach and also scientifically proved that it has the huge impact to alter the physicochemical properties of various non-living and living object(s) [6-9]. The Trivedi Effect® is natural and the only scientifically proven phenomenon in which a person can harness this inherently intelligent energy from the Universe and transmit it anywhere on the planet. It is believed that the Trivedi Effect® act through the possible mediation of neutrinos oscillation [10]. A unique para-dimensional electromagnetic field exists around the body of every living organism which produces due to the continuous movements of the charged particles, ions, cells, blood/lymph flow, heart function, and brain functions in the body known as the "Biofield". The Biofield based Energy Therapies (energy medicine) have been reported with significantly beneficial outcomes against various disease conditions [11].

The National Institute of Health (NIH) and the National Centre for Complementary and Alternative Medicine (NCCAM) recommend and included the Energy therapy under the Complementary

and Alternative Medicine (CAM) category along with traditional Chinese herbs and medicines, Ayurvedic medicine, naturopathy, homeopathy, yoga, acupuncture, acupressure, meditation, Tai Chi, Qi Gong, chiropractic/osteopathic manipulation, healing touch, Reiki, deep breathing, special diets, massage, progressive relaxation, relaxation techniques, guided imagery, movement therapy, hypnotherapy, pilates, Rolfing structural integration, mindfulness, cranial sacral therapy, aromatherapy, and applied prayer; which has been accepted by the most of the U.S.A. population [12,13]. In this regard, the Trivedi Effect®-Consciousness Energy Healing Treatment also significantly altered the physicochemical and thermal properties of metals, ceramics, polymers, organic compounds, pharmaceuticals, nutraceuticals [14-19], improved productivity of crops and livestock [20,21], inhibit the growth of microbes and cancer cells [22,23]. The current study was designed and evaluated the effect of the Trivedi Effect®-Consciousness Energy Healing Treatment on chromium trioxide using particle size analysis (PSA), powder X-ray diffraction (PXRD), and differential scanning calorimetry (DSC) analytical techniques.

## Materials and Methods

### Chemicals and reagents

The chromium (VI) oxide ( $\text{CrO}_3$ ) powder sample was purchased from Sigma Aldrich, India. All other chemicals used during the experiments were of analytical grade also procured from India.

### Consciousness energy healing treatment strategies

The  $\text{CrO}_3$  powder test sample was divided into two parts. One part of the test sample was provided the Trivedi Effect®-Consciousness energy healing treatment remotely under standard laboratory conditions for 3 minutes, known as the treated sample. Biofield Energy Treatment was provided through the healer's unique energy transmission process by a renowned Biofield Energy Healer, Gopal Nayak, India, to one of the test sample. The second part of the test item was considered as a control sample (no Biofield Energy Treatment was provided). Further, the control sample was treated with a "sham" healer for the better comparison with the results of the Biofield Energy Treated sample. In this case, the "sham" healer did not have any knowledge about the Biofield Energy Treatment. After the treatment, both the Biofield Energy Treated and untreated samples were kept in sealed conditions and characterized using PSA, PXRD, and DSC analytical techniques.

### Characterization

**Particle size analysis (PSA):** The particle size analysis of  $\text{CrO}_3$  powder was performed on Malvern Mastersizer 2000, from the UK with a detection range between  $0.01\mu\text{m}$  to  $3000\mu\text{m}$  using wet method [24,25]. The sample unit (Hydro MV) was filled with a dispersant medium (sunflower oil) and the stirrer operated at 2500 rpm. The PSA analysis of  $\text{CrO}_3$  was performed to obtain the average particle size distribution. Where  $d$  ( $0.1\mu\text{m}$ ),  $d$  ( $0.5\mu\text{m}$ ),  $d$  ( $0.9\mu\text{m}$ ) represent particle diameter corresponding to 10%, 50%, and 90% of the cumulative distribution.  $D$  (4,3) represents the average mass-volume diameter, and SSA is the specific surface area ( $\text{m}^2/\text{g}$ ). The calculations were done by using software Mastersizer Ver. 5.54.

The percent change in particle size ( $d$ ) for  $\text{CrO}_3$  powder at below 10% level ( $d_{10}$ ), 50% level ( $d_{50}$ ), 90% level ( $d_{90}$ ), and  $D$  (4,3) was calculated using the following equation 1:

$$\% \text{ change in particle size} = \frac{[d_{\text{Treated}} - d_{\text{Control}}]}{d_{\text{Control}}} \times 100 \quad (1)$$

Where  $d_{\text{Control}}$  and  $d_{\text{Treated}}$  are the particle sizes ( $\mu\text{m}$ ) for at below 10% level ( $d_{10}$ ), 50% level ( $d_{50}$ ) and 90% level ( $d_{90}$ ) of the control and the Biofield Energy Treated samples, respectively.

The percent change in surface area ( $S$ ) was calculated using the following equation 2:

$$\% \text{ change in surface area} = \frac{[S_{\text{Treated}} - S_{\text{Control}}]}{S_{\text{Control}}} \times 100 \quad (2)$$

Where  $S_{\text{Control}}$  and  $S_{\text{Treated}}$  are the surface area of the control and the Biofield Energy Treated  $\text{CrO}_3$ , respectively.

**Powder X-ray diffraction (PXRD) analysis:** The PXRD analysis of  $\text{CrO}_3$  was performed with the help of Rigaku Mini Flex-II Desktop X-ray diffractometer (Japan) [26,27]. The  $\text{CuK}\alpha$  radiation source tube output voltage used was 30kV, and tube output current was 15mA. Scans were performed at room temperature. The average size of individual crystallites was calculated from PXRD data using the Scherrer's formula (3):

$$G = k\lambda / \beta \cos\theta \quad (3)$$

Where  $k$  is the equipment constant (0.94),  $G$  is the crystallite size in nm,  $\lambda$  is the radiation wavelength (0.154056 nm for  $\text{K}\alpha 1$  emission),  $\beta$  is the full-width at half maximum (FWHM), and  $\theta$  is the Bragg angle [28].

The percent change in crystallite size ( $G$ ) of  $\text{CrO}_3$  was calculated using the following equation 4:

$$\% \text{ change in crystallite size} = \frac{[G_{\text{Treated}} - G_{\text{Control}}]}{G_{\text{Control}}} \times 100 \quad (4)$$

Where  $G_{\text{Control}}$  and  $G_{\text{Treated}}$  are the crystallite size of the control and the Biofield Energy Treated samples, respectively.

**Differential scanning calorimetry (DSC):** The DSC analysis of  $\text{CrO}_3$  was performed with the help of DSC Q200, TA instruments. The sample of ~1-3 mg was loaded to the aluminium sample pan at a heating rate of  $10^\circ\text{C}/\text{min}$  from  $30^\circ\text{C}$  to  $350^\circ\text{C}$  [24,25]. The % change in melting point ( $T$ ) was calculated using the following equation 5:

$$\% \text{ change in melting point} = \frac{[T_{\text{Treated}} - T_{\text{Control}}]}{T_{\text{Control}}} \times 100 \quad (5)$$

Where  $T_{\text{Control}}$  and  $T_{\text{Treated}}$  are the melting point of the control and treated samples, respectively.

The percent change in the latent heat of fusion ( $\Delta H$ ) was calculated using the following equation 6:

$$\% \text{ change in the latent heat of fusion} = \frac{[\Delta H_{\text{Treated}} - \Delta H_{\text{Control}}]}{\Delta H_{\text{Control}}} \times 100 \quad (6)$$

Where  $\Delta H_{\text{Control}}$  and  $\Delta H_{\text{Treated}}$  are the latent heat of fusion of the control and the Biofield Energy Treated  $\text{CrO}_3$ , respectively.

## Results and Discussion

### Particle size analysis (PSA)

The particle size and surface area data of both the control and the Biofield Energy Treated  $\text{CrO}_3$  powder are presented in Table 1.

The particle size values of the control sample at  $d_{10}$ ,  $d_{50}$ ,  $d_{90}$ , and  $D(4,3)$  were 172.19  $\mu\text{m}$ , 321.58  $\mu\text{m}$ , 549.35  $\mu\text{m}$ , and 341.53  $\mu\text{m}$  respectively. Similarly, the particle sizes of the treated  $\text{CrO}_3$  at  $d_{10}$ ,  $d_{50}$ ,  $d_{90}$  and  $D(4,3)$  were 176.31  $\mu\text{m}$ , 336.12  $\mu\text{m}$ , 573.63  $\mu\text{m}$ , and 355.7  $\mu\text{m}$  respectively. The particle size values in the treated  $\text{CrO}_3$  powder was increased at  $d_{10}$ ,  $d_{50}$ ,  $d_{90}$  and  $D(4,3)$  by 2.39%, 4.52%, 4.42%, and 4.15%, respectively compared to the control sample. Thus, the specific surface area (SSA) of the treated  $\text{CrO}_3$  powder (0.0224  $\text{m}^2/\text{g}$ ) was decreased by 4.27% compared with the control sample (0.0234  $\text{m}^2/\text{g}$ ). The results indicated that the Biofield

Energy Treatment might be responsible for reducing internal force for increasing the particle size of  $\text{CrO}_3$  sample, hence decreasing the surface area significantly. Increase in the particle size of the compound may help in enhancing the appearance, shape, and powder flowability of the compound [29,30]. Hence, the Trivedi Effect®-Consciousness Energy Healing Treated  $\text{CrO}_3$  might improve the powder flowability, lower solubility, lower the absorption, and lower toxicity due to inhalation, ingestion, contact to skin and eye, chronic exposure, and aggravation of pre-existing conditions.

**Table 1:** Particle size distribution of the control and the Biofield Energy Treated  $\text{CrO}_3$  powder.

Parameter	$d_{10}$ ( $\mu\text{m}$ )	$d_{50}$ ( $\mu\text{m}$ )	$d_{90}$ ( $\mu\text{m}$ )	$D(4,3)$ ( $\mu\text{m}$ )	SSA ( $\text{m}^2/\text{g}$ )
Control	172.19	321.58	549.35	341.53	0.0234
Biofield Treated	176.31	336.12	573.63	355.7	0.0224
Percent change* (%)	2.39	4.52	4.42	4.15	-4.27

$d_{10}$ ,  $d_{50}$  and  $d_{90}$ : particle diameter corresponding to 10%, 50% and 90% of the cumulative distribution;  $D(4,3)$ : The average mass-volume diameter; SSA: the specific surface area.

\*Denotes the percentage change in the Particle size distribution of the Biofield Energy Treated sample with respect to the control sample.

### Powder X-ray diffraction (PXRD) analysis

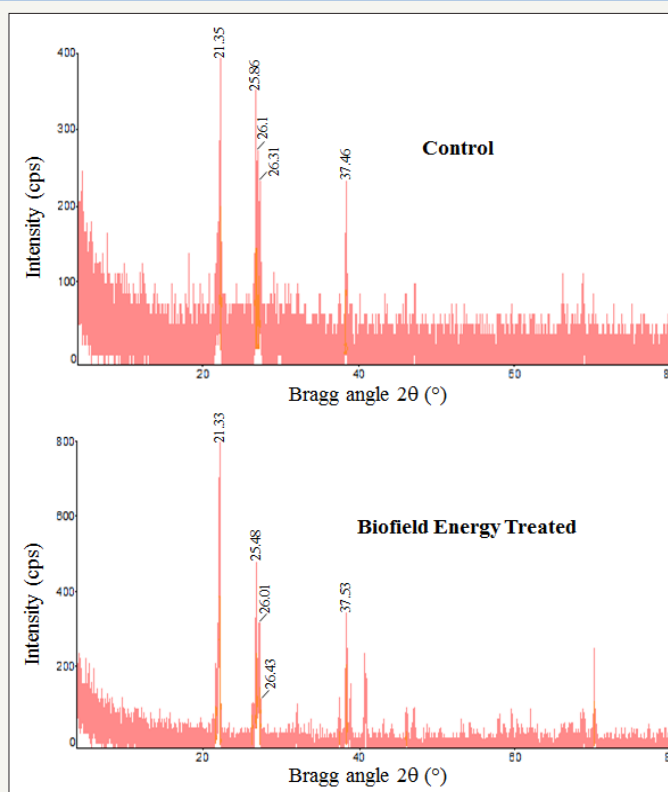


**Figure 1:** PXRD diffractograms of the control and the Biofield Energy Treated  $\text{CrO}_3$  powder.

The PXRD diffractograms of both the control and the Biofield Energy Treated  $\text{CrO}_3$  powder samples showed the sharp and intense peaks (Figure 1) indicating both the samples were crystalline. The control sample showed peaks at Bragg's angle ( $2\theta$ ) equal to 21.35°, 25.86°, 26.1°, 26.31° and 37.46° in the chromatogram (Figure 1). Similarly, the Biofield Energy Treated sample showed peaks at

Bragg's angle ( $2\theta$ ) equal to 21.33°, 25.48°, 26.01°, 26.43° and 37.53° in the chromatogram (Figure 1). The highest peak intensity of both the samples was found at  $2\theta$  equal to 21.3° (Table 2). Overall, the peak intensities of the treated  $\text{CrO}_3$  were significantly altered ranging from -73.48% to 121.5% compared to the control sample (Table 2). As well, the crystallite sizes of the Biofield Energy Treated

sample at  $2\theta$  were significantly altered ranging from -38.7% to 167.39% compared to the control sample (Table 2). Overall, the average crystallite size of the Trivedi Effect®-Consciousness Energy

Healing Treated (672.6 nm) was increased by 4.25% compared with the control sample (645.2 nm).

**Table 2:** PXRD data for the control and the Biofield Energy Treated  $\text{CrO}_3$  powder.

Entry No.	Bragg angle ( $2\theta$ )		Peak Intensity (%)			Crystallite size (G, nm)		
	Control	Treated	Control	Treated	% change <sup>a</sup>	Control	Treated	% change <sup>b</sup>
1	21.35	21.33	50	98	96	564	393	-30.32
2	25.86	25.48	23	6.1	-73.48	552	1476	167.39
3	26.1	26.01	16	50	212.5	832	510	-38.7
4	26.31	26.43	23	41	78.26	402	364	-9.45
5	37.46	37.53	13.7	39	184.67	876	620	-29.22
6	Average crystallite size					645.2	672.6	4.25

<sup>a</sup>denotes the percentage change in the peak intensity of the Biofield Energy Treated sample with respect to the control sample;

<sup>b</sup>denotes the percentage change in the crystallite size of the Biofield Energy Treated sample with respect to the control sample.

The results suggested that the crystallite sizes and peak intensities of the Trivedi Effect®-Consciousness Energy Healing Treated sample were significantly altered compared to the control sample. The peak intensity of the crystalline compound changes according to the crystal morphology, and alterations in the PXRD pattern is the proof of polymorphic transitions [31-33]. The Trivedi Effect® Treatment might have produced a new polymorphic

form of  $\text{CrO}_3$  via neutrinos oscillation [10]. The change in the polymorphic forms of a compound have the significant effects on their physicochemical and thermal properties like melting point, energy, stability, and solubility [34,35]. Therefore, the Biofield Energy Treated  $\text{CrO}_3$  would be more useful for the industries using it as a raw material for manufacturing.

#### Differential scanning calorimetry (DSC) analysis

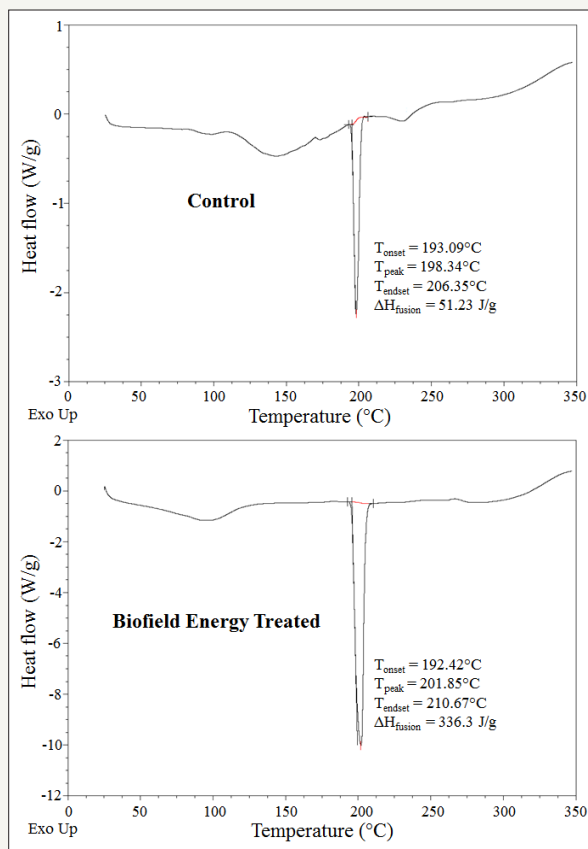


**Figure 2:** DSC thermograms of the control and the Biofield Energy Treated  $\text{CrO}_3$  powder.



The control and the Biofield Energy Treated  $\text{CrO}_3$  sample showed sharp endothermic peaks at 198.34 °C and 201.85 °C, respectively (Figure 2) in the thermograms. The thermal analysis data of  $\text{CrO}_3$  indicated that the thermal behavior of the Biofield Energy Treated sample was significantly altered compared to the control sample (Table 3). The melting point of the Biofield Energy Treated  $\text{CrO}_3$  sample was increased by 1.77% compared to the control sample (Table 3). The latent heat of fusion ( $\Delta H_{\text{fusion}}$ ) of the Biofield Energy Treated  $\text{CrO}_3$  powder (336.3J/g) was significantly increased by 556.45% compared to the control sample (51.23J/g) (Table 3). The change in the latent heat of fusion can be attributed to the alteration in the molecular chains and the crystal structure [36]. Therefore, Gopal Nayak's Biofield Energy Treatment (the Trivedi Effect®) might strengthen intermolecular bond/chains and crystal structure of  $\text{CrO}_3$  which improved the thermal stability of the treated sample compared with the control sample.

**Table 3:** DSC data for both control and the Biofield Energy Treated samples of  $\text{CrO}_3$  powder.

Sample	Melting point (°C)	$\Delta H$ (J/g)
Control Sample	198.34	51.23
Biofield Energy Treated	201.85	336.3
% Change*	1.77	556.45

$\Delta H$ : Latent heat of fusion.

\*Denotes the percentage change of the Biofield Energy Treated  $\text{CrO}_3$  powder with respect to the control sample.

## Conclusion

These study results suggest that the Trivedi Effect®-Consciousness Energy Healing Treatment has a significant impact on the surface area, particle size, crystallite size, and thermal properties of  $\text{CrO}_3$ . The particle size values of the Biofield Energy Treated  $\text{CrO}_3$  were increased by 2.39%, 4.52%, 4.42%, and 4.15% at  $d_{10}$ ,  $d_{50}$ ,  $d_{90}$  and D (4,3), respectively compared to the control sample. Thus, the SSA of the Biofield Energy Treated sample was decreased by 4.27% compared with the control sample. The PXRD peak intensities of the Biofield Energy Treated  $\text{CrO}_3$  were significantly altered ranging from -73.48% to 212.5% compared with the control sample. Similarly, the crystallite sizes of the Biofield Energy Treated sample were significantly altered ranging from -38.7% to 167.39% compared to the control sample. However, the average crystallite size of the Biofield Energy Treated sample was increased by 4.25% compared with the control sample. The melting point of the Biofield Energy Treated  $\text{CrO}_3$  was slightly increased by 1.77% compared with the control sample. The  $\Delta H_{\text{fusion}}$  of the Biofield Energy Treated sample was significantly increased by 556.45% compared with the control sample. The Trivedi Effect®-Consciousness Energy Healing Treatment might produce a new polymorphic form of  $\text{CrO}_3$  which would be better powder flowability and lower solubility; hence it will show the lower absorption and toxicity on inhalation, ingestion, contact to skin and eye, chronic exposure, and aggravation of pre-existing conditions. As well Biofield Energy Treated  $\text{CrO}_3$  sample would be very useful for the ceramic industry manufacturing the

synthetic rubies, stripping agent of anodic coatings, aerospace parts, etc.

## Acknowledgement

The authors are grateful to Central Leather Research Institute, SIPRA Lab. Ltd., Trivedi Science, Trivedi Global, Inc., Trivedi Testimonials, and Trivedi Master Wellness for their assistance and support during this work.

## References

1. <http://www.chemicaland21.com/industrialchem/inorganic/CHROMIUM%20TRIOXIDE.htm>
2. [https://en.wikipedia.org/wiki/Chromium\\_trioxide](https://en.wikipedia.org/wiki/Chromium_trioxide)
3. Anger G, Halstenberg J, Hochgeschwender K, Scherhag C, Korallus U, et al. (2000) Chromium compounds. Ullmann's Encyclopedia of Industrial Chemistry.
4. MacInnis, Daniel (1973) Synthetic gem and allied crystal manufacture. Park Ridge, Noyes Data Corporation, NJ, USA.
5. <http://hazard.com/msds/mf/baker/baker/files/c4400.htm>
6. Trivedi MK, Branton A, Trivedi D, Shettigar H, Nayak G, et al. (2015) Assessment of antibiogram of multidrug-resistant isolates of *Enterobacter aerogenes* after biofield energy treatment. J Pharma Care Health Sys 2: 145.
7. Nayak G, Altekar N (2015) Effect of a biofield treatment on plant growth and adaptation. J Environ Health Sci 1: 1-9.
8. Trivedi MK, Branton A, Trivedi D, Nayak G, Sethi KK, et al. (2016) Isotopic abundance ratio analysis of biofield energy treated indole using gas chromatography-mass spectrometry. Science Journal of Chemistry 4: 41-48.
9. Dabhade VV, Tallapragada RMR, Trivedi MK (2009) Effect of external energy on the atomic, crystalline, and powder characteristics of antimony and bismuth powders. Bulletin of Materials Science 32: 471-479.
10. Trivedi MK, Mohan TRR (2016) Biofield energy signals, energy transmission and neutrinos. American Journal of Modern Physics 5: 172-176.
11. Rubik B, Muehsam D, Hammerschlag R, Jain S (2015) Biofield science and healing: history, terminology, and concepts. Glob Adv Health Med 4: 8-14.
12. Barnes PM, Bloom B, Nahin RL (2008) Complementary and alternative medicine use among adults and children: United States, 2007. Natl Health Stat Report 12: 1-23.
13. Koithan M (2009) Introducing complementary and alternative therapies. J Nurse Pract 5(1): 18-20.
14. Trivedi MK, Tallapragada RM (2008) A transcendental to changing metal powder characteristics. Metal Powder Report 63(9): 22-28, 31.
15. Trivedi MK, Nayak G, Patil S, Tallapragada RM, Latiyal O (2015) Studies of the atomic and crystalline characteristics of ceramic oxide nano powders after bio field treatment. Ind Eng Manage 4: 161.
16. Trivedi MK, Nayak G, Patil S, Tallapragada RM, Mishra R (2015) Influence of biofield treatment on physicochemical properties of hydroxyethyl cellulose and hydroxypropyl cellulose. J Mol Pharm Org Process Res 3: 126.
17. Trivedi MK, Branton A, Trivedi D, Nayak G, Panda P, et al. (2016) Determination of isotopic abundance of  $^{13}\text{C}/^{12}\text{C}$  or  $^2\text{H}/^1\text{H}$  and  $^{18}\text{O}/^{16}\text{O}$  in biofield energy treated 1-chloro-3-nitrobenzene (3-CNB) using gas chromatography-mass spectrometry. Science Journal of Analytical Chemistry 4: 42-51.

18. Trivedi MK, Patil S, Shettigar H, Bairwa K, Jana S (2015) Spectroscopic characterization of biofield treated metronidazole and tinidazole. *Med chem* 5: 340-344.
19. Branton A, Jana S (2017) Effect of the biofield energy healing treatment on the pharmacokinetics of 25-hydroxyvitamin D<sub>3</sub> [25(OH)D<sub>3</sub>] in rats after a single oral dose of vitamin D<sub>3</sub>. *American Journal of Pharmacology and Phytotherapy* 2: 11-18.
20. Trivedi MK, Branton A, Trivedi D, Nayak G, Mondal SC, et al. (2015) Evaluation of plant growth, yield and yield attributes of biofield energy treated mustard (*Brassica juncea*) and chick pea (*Cicer arietinum*) seeds. *Agriculture, Forestry and Fisheries* 4: 291-295.
21. Trivedi MK, Branton A, Trivedi D, Nayak G, Mondal SC, et al. (2015) Effect of biofield treated energized water on the growth and health status in chicken (*Gallus gallus domesticus*). *Poult Fish Wildl Sci* 3: 140.
22. Trivedi MK, Branton A, Trivedi D, Shettigar H, Nayak G, et al. (2015) Assessment of antibiogram of multidrug-resistant isolates of *Enterobacter aerogenes* after biofield energy treatment. *J Pharma Care Health Sys* 2: 145.
23. Trivedi MK, Patil S, Shettigar H, Mondal SC, Jana S (2015) The potential impact of biofield treatment on human brain tumor cells: A time-lapse video microscopy. *J Integr Oncol* 4: 141.
24. Trivedi MK, Sethi KK, Panda P, Jana S (2017) A comprehensive physicochemical, thermal, and spectroscopic characterization of zinc (II) chloride using X-ray diffraction, particle size distribution, differential scanning calorimetry, thermogravimetric analysis/differential thermogravimetric analysis, ultraviolet-visible, and Fourier transform-infrared spectroscopy. *Int J Pharm Investig* 1(1): 33-40.
25. Trivedi MK, Sethi KK, Panda P, Jana S (2017) Physicochemical, thermal and spectroscopic characterization of sodium selenate using XRD, PSD, DSC, TGA/DTG, UV-vis, and FT-IR. *Marmara Pharmaceutical Journal* 21(2): 311-318.
26. Desktop X-ray Diffractometer "MiniFlex+" (1997) The Rigaku Journal 14: 29-36.
27. Zhang T, Paluch K, Scalabrino G, Frankish N, Healy AM, et al. (2015) Molecular structure studies of (1S,2S)-2-benzyl-2,3-dihydro-2-(1Hinden-2-yl)-1H-inden-1-ol. *J Mol Struct* 1083: 286-299.
28. Langford JJ, Wilson AJC (1978) Scherrer after sixty years: A survey and some new results in the determination of crystallite size. *J Appl Cryst* 11: 102-113.
29. Mosharraf M, Nystrom C (1995) The effect of particle size and shape on the surface specific dissolution rate of micro sized practically insoluble drugs. *Int J Pharm* 122(1-2): 35-47.
30. Buckton G, Beezer AE (1992) The relationship between particle size and solubility. *Int J Pharmaceutics* 82(3): R7-R10.
31. Inoue M, Hirasawa I (2013) The relationship between crystal morphology and XRD peak intensity on CaSO<sub>4</sub>·2H<sub>2</sub>O. *J Crystal Growth* 380: 169-175.
32. Raza K, Kumar P, Ratan S, Malik R, Arora S (2014) Polymorphism: The phenomenon affecting the performance of drugs. *SOJ Pharm Pharm Sci* 1: 10.
33. Brittain HG (2009) Polymorphism in pharmaceutical solids in *Drugs and Pharmaceutical Sciences*, volume 192, 2<sup>nd</sup> Edn, Informa Healthcare, Inc., New York, USA.
34. Censi R, Martino PD (2015) Polymorph impact on the bioavailability and stability of poorly soluble drugs. *Molecules* 20(10): 18759-18776.
35. Blagden N, DeMatas M, Gavan PT, York P (2007) Crystal engineering of active pharmaceutical ingredients to improve solubility and dissolution rates. *Adv Drug Deliv Rev* 59(7): 617-630.
36. Zhao Z, Xie M, Li Y, Chen A, Li G, et al. (2015) Formation of curcumin nanoparticles *via* solution-enhanced dispersion by supercritical CO<sub>2</sub>. *Int J Nanomedicine* 10: 3171-3181.



Creative Commons Attribution 4.0  
International License

For possible submissions Click Here

Submit Article



## Research & Development in Material Science

### Benefits of Publishing with us

- High-level peer review and editorial services
- Freely accessible online immediately upon publication
- Authors retain the copyright to their work
- Licensing it under a Creative Commons license
- Visibility through different online platforms